Feasibility of a High Efficiency Solar Air Conditioner Powered by DC Current

Mohammad Kazemi Bidhendi *[1] ,Alireze Derakshan [2]

[1] Faculty of Electrical and Computer Engineering, Islamic Azad University of Karaj, Alborz, Iran
[2] Institute of Separation Science and Technology, Friedrich-Alexander-Universität Erlangen, Germany
* Corresponding author; kazemi_bidhendi@yahoo.com

Abstract

The feasibility of direct use of photovoltaic energy to supply cooling demand of a building is investigated at a demonstration site through its design, installation and evaluation. The cooling is accomplished by using a novel method of energy supply, including photovoltaic panels, electrically driven solar-assisted heat pump, in-house developed inverter and thermal energy storage system. The refrigeration unit is based on a variable speed heat pump, which is supplied by direct current (DC) from photovoltaic panels. In order to provide appropriate current and voltage with high energy transform efficiency, a novel inverter is developed. While in conventional systems four energy transform stages are needed to supply a variable speed heat pump, by this method conversions are reduced to two. In addition, a modular structure of the inverter improves the transformation efficiency, particularly in partial load condition. Although, using this technology reduces the number of energy transformations and losses, but intermittency and variability of PV power will be transferred to the heat pump and the cooling power accordingly. Therefore, a kind of energy stabilizer system is necessary to control the energy fluctuation. Hence, a 30 m^3 water tank is used as the thermal energy storage system. The heat pump can be fed simultaneously by both PV and grid power through two separate interfaces. Thus, no additional backup system is needed. The results show that the solar fraction for a sunny and a cloudy day is 69 % and 20 % respectively which is higher than average similar systems due to the simultaneous usage of PV and grid power without any auxiliary backup system.

Keywords: solar cooling system, variable speed heat pump, DC/DC inverter
Article history: Submitted 29-Mar-2022; Revised 08-May-2022; Accepted 10-May-2022. Article Type: Research paper

https://doi.org/10.30495/ijsee.2022.1955668.1191

1. Introduction

Residential and commercial buildings account for a high share of energy consumption; in the United States, more than one third of the total primary energy is consumed by this sector [1]. In addition, nowadays energy demand in the buildings is increasing dramatically due to the continued rise of living comfort conditions. In certain areas of Europe the energy consumption resulting from the use of air conditioning systems can reach half of the total consumption of buildings [2].

World energy demand and CO_2 emissions is expected to rise about 60% by 2030 with respect to the beginning of this century [3][26]. Shortage of energy resources and negative environmental impact encourage researchers to develop novel strategies with renewable energies and optimized levels of efficiency to lessen the energy consumption. Recently, many experimental, theoretical, analytical, economical and numerical, investigations about novel cooling systems based on solar energy have been performed. The main advantage of solar-assisted cooling systems is the fact that solar irradiation and cooling demand are typically in good temporal and geographical coincidence.

Although most of the efforts are concentrated on thermally driven solar air conditioners [27][28] [3-10], technically it is proven that solar electric refrigeration systems constitute the most efficient cooling system[29]. Despite of high solar fraction (SF) in thermally driven solar cooling systems, they suffer from some drawbacks. The coefficient of performance (COP) of the absorption system is in the range of 0.5-0.8 and 1.1-1.4 for single effect and double effect machines, respectively while the COP of vapor compression air conditioner systems is around 3-5. In addition, though the running cost of

the absorption refrigeration system is less than of the vapor compression system, its initial capital cost is much higher and because of complex working principles, it is difficult to integrate thermally driven systems in small or even medium size buildings. Furthermore, a significant portion of useful solar energy will be wasted through the piping and system preheating due to overnight heat loss [11].

Solar electric cooling systems have higher energy saving potential, particularly the grid coupled systems [12].

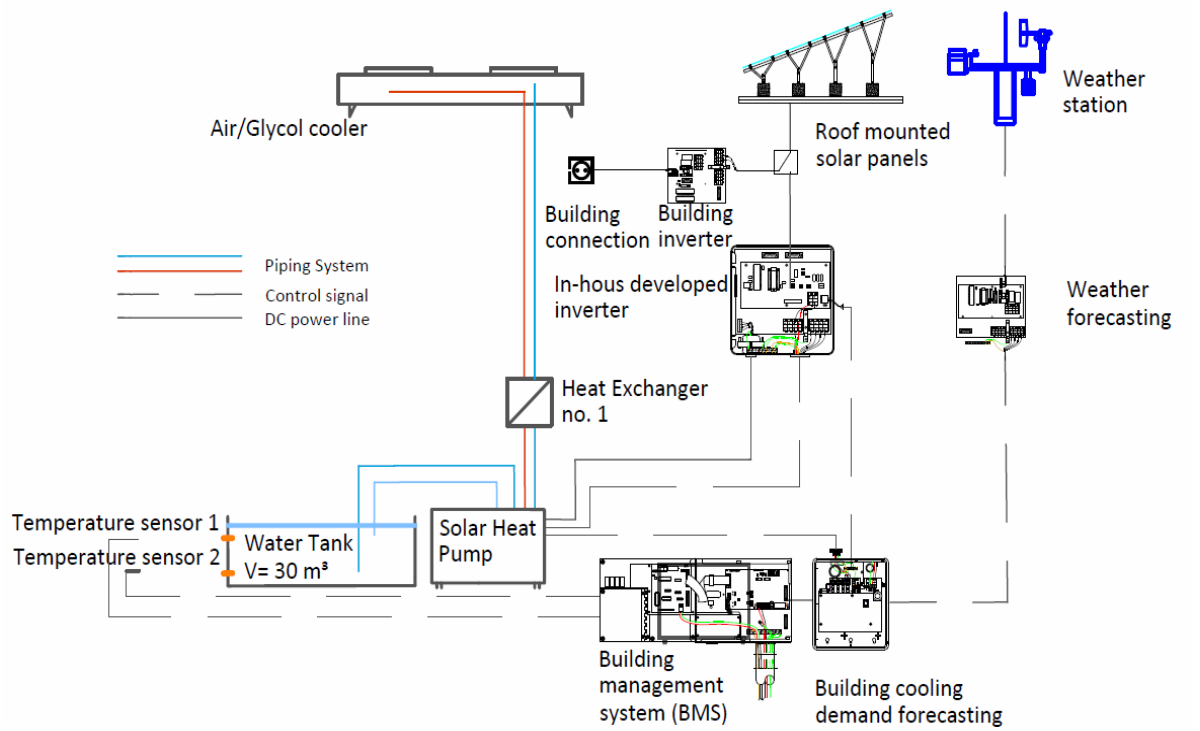

Fig. 1. Simplified Process and Instrumentation Diagram (P&ID) of the solar cooling system.

Fong et al. compared five types of solar cooling systems in a comparative study for a subtropical city. The solar cooling systems included solar electric compression refrigeration and different types of thermally driven systems, i.e. solar mechanical compression refrigeration, solar absorption refrigeration, solar adsorption refrigeration and solar solid desiccant cooling. The main indicators including solar fraction, coefficient of performance (COP), solar thermal gain, primary energy consumption, types of installation strategy and types of solar collectors were compared. Through this comparative study, it was found that the solar electric compression refrigeration had the highest energy saving potential [13]. Eicker et al. also compared the performance of a fixed speed solar heat pump with a solar single effect absorption system through simulation. Different building load scenarios and climate conditions were simulated. It was concluded that the solar heat pump, in feed-in analysis, has higher primary energy saving in all modelling scenarios [14].

The efficiency is even expected to be higher in variable speed (electrically driven) systems. A data set including energy efficiency, price and average electricity consumption of different electrically driven air conditioners was collected from China's market. The samples cover 527 models of air conditioners across 17 brands, among which 307 models are fixed-frequency air conditioners and 220 models are variable speed systems. The models are categorized in three levels according to the rated cooling capacity (CC); CC ≤ 4500-Watt, 4500 Watt < CC ≤ 7100 Watt and 7100 Watt < CC ≤ 14000 Watt. For all levels, the average electricity consumption of variable speed systems is at least 15% less than the similar level of fixed speed model [15]. The American Society of Heating, Refrigeration and Air-Conditioning Engineers (ASHRAE) showed that, on average, most locations in the United States see the need for 100 percent capacity less than 5 percent of the year, and see the need for part-load capacity (approximately 75 percent of full load) for 60 to 80 percent of the year [16].

2. Proposed system

While the majority of the electrically driven solar air conditioner are based on fixed-speed compressor systems [17-23], the proposed concept consists of a variable speed compressor.

Variable speed air conditioners are the state-of-art technology in the HVAC industry which leads to a significant energy saving [24]. Furthermore, it offers more noiseless operation and more flexible control. This work presents a newly-developed air conditioner based on a variable speed electric compression system (heat pump) which is supplied by direct current (DC) from photovoltaic panels. The process and instrumentation diagram of the demonstration site is depicted in Fig. 1. The heat pump is powered by 600 V_{DC}. To the best of our knowledge no similar system has been designed in this range. Aguilar et al. developed a hybrid (grid + PV) fixed speed heat pump which was fed with 21 V_{DC} [2]. In comparison to the conventional solar variable speed systems, three novel concepts are developed:

- Four energy transform stages are necessary in a conventional system i.e. two stages at PV panel inverter and two additional stages at the VFD (Variable Frequency Driver) of the heat pump. The proposed method reduces the conversion stages to two; DC/DC in the PV system and DC/AC in the heat pump (see Fig. 2). In addition, modular structure of the DC/DC converter improves the efficiency especially at partial loads.
- In conventional systems, compressor speed changes according to the heating/cooling load. In the proposed concept, a new algorithm is developed for the control system. Thereby, compressor speed will be adjusted according to the available solar energy. Hence, heat pump follows the PV power curve, which maximizes the usage of available solar energy. When solar energy is more than the load, surplus energy will be stored in the water tank. The tank provides energy during the periods when PV power is deficient.
- In contrast to the conventional VFDs, heat pump can be fed by both PV and grid power at the same time. By this method, PV power can be immediately replaced with grid during the sharp PV reduction in order to protect the compressor and to provide continuing energy production. Therefore, no backup system is needed.

Technical feasibility of this concept is investigated and demonstrated in this work.

3. Description of components

A) Energy stabilizing

A 30 m^3 water tank is used as the thermal energy storage system. The stored energy in the tank stabilizes the solar energy fluctuations and provides enough energy for low irradiation days.

Tank efficiency is measured between June and July 2020. The demonstration site is a commercial building and the cooling system stops at 8:00pm every evening and starts at 8:00am the next morning. Thermal behavior of the tank during these 12 hours is monitored to calculate the performance, because there is no external input/output energy in this period. Two sensors, at the top and the bottom of the tank, measure the water temperature every 8 minutes. The average tank efficiency between June and July is 93.9 % and 88.2 % based on top and bottom sensor respectively. There are two reasons for the higher efficiency at the top of the tank:

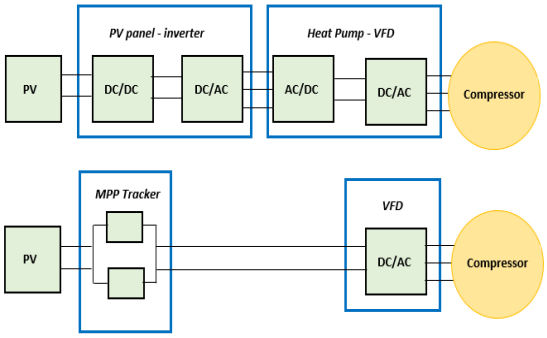

Fig. 2. Above: energy transform stages in a conventional solar variable speed heat pump. Bottom: energy transform stages in the proposed method; half of the transform stages are removed. In addition, modular structure of the DC/DC converter improves the efficiency especially at partial loads.

-Water temperature is higher at the top; therefore, the heat exchange rate is lower.

-The air gap between water surface and tank ceiling acts as an additional insulation while water is directly in contact with the tank surface at the bottom.

Fig. 3 shows the water temperature in the tank for a typical day and the efficiency of tank for different days. The tank efficiency based on bottom sensor drops if ambient temperature increases, while the efficiency of tank at top is less sensitive to the outside temperature. After turning off the cooling system, the water temperature decreases at the beginning, which shows the inherent inertia of the tank. Same circumstance happens at the start point, which is faster because of the external input energy.

The intake connection of the cooling system is installed at the same height as the bottom sensor. Hence, it is more reasonable to work with this efficiency.

B) Solar system

The solar system involves 18 panels with a name-plate DC power of 250 W_p. In order to find the optimum inclination angle, the PV system is simulated at 15°, 25°, 35° and 45°. The annual AC

power is 4150, 4200, 4180 and 4000 kWh/year, respectively. Therefore, a roof free-standing structure with an inclination of 25° is used to install the panels.

C) Variable Speed Heat pump (VSHP)

The term "variable-speed " refers to the ability of heat pump to vary the compressor speed. Therefore, this kind of heat pump can operate far more efficiently because its output varies according to the demand, rather than running at a full or a single reduced capacity. Current VSHPs on the market provide operating ranges from 100% capacity down to about 40%, for this new heat pump we used a novel compressor which can work even at levels lower than 20%. Hence, more solar energy can be used by heat pump.

The essential components of a VSHP are evaporator, scroll compressor, condenser, electrical expansion valve, chilled water pump, condenser water pump and Variable Frequency Drive (VFD). In detail, as presented in Fig. 4, the evaporator exchanges the heat between the water to be cooled and the refrigerant (R410a). After the compressor raises the refrigerant temperature and pressure, the heat collected in both the evaporator and the compressor is removed from the refrigerant to a hot water cycle. From the hot water cycle the heat is transferred to the ambient air by an air/water cooler. A commercial water/ water heat pump (Heliotherm HP12S16W-M) is used in this work, the heat pump technical data is shown in Table 1.

In order to control the compressor speed, the VFD varies the frequency supplied to the compressor. Frequency is directly related to the motor's speed. The first stage of VFD is a Converter, which receives AC voltage with 400V and produces DC voltage with an AC ripple. The AC ripple on the DC bus is typically less than 3 Volts and the DC voltage runs between approximately 580V and 600V. In the second stage, by using a capacitor on the DC bus, the AC ripple can be removed and deliver a smooth DC voltage. The last stage is the DC-to-AC inverter which generates AC current with the desired frequency. The output from the VFD is a "rectangular" wave form. This rectangular waveform would not be a good choice for a general-purpose distribution system, but is perfectly adequate for a compressor. The internal circuit and output of each stage are shown in Fig. 5.

D) Inverter

To transfer the energy from the PV-Panels to the heat pump, a novel DC/DC inverter is developed in this project. The first stage of DC/DC inverter is the maximum power point (MPP) tracking system which regulates the PV-Panels output to the point of maximum power. This maximum power point is

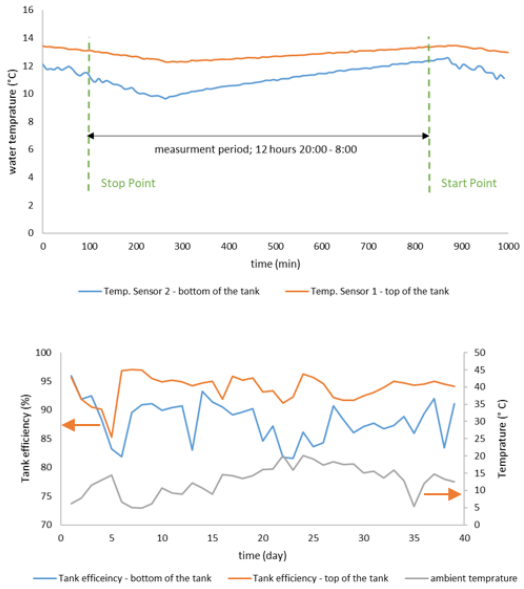

Fig. 3. Tank performance. Top: water temperature in a typical day with tank efficiency of 91.7 % and 86.1 % based on the top and the bottom sensor. Temperature changes between 9.63 °C and 12.85 °C at the bottom and between 12.27 °C and 13.48 °C at the top of the tank. Bottom: tank efficiency between June and July 2020.

certainly, the target of PV operation. The second stage of inverter is the DC-Bus regulator which is directly connected to the DC-Bus of VFD (see Fig. 5). The regulator monitors and adjusts the output of inverter on 600 V_{DC}. In order to increase the efficiency, the DC/DC inverter is composed of two small inverters connected in parallel which create a modular structure. Each inverter is able to be switched on and off depending on the power flow. i.e. in partial loads just one inverter is on and thus the losses will be reduced. Furthermore, the modular structure enables scalability. An integrated control system regulates the inverter performance and communicates with other equipment such as heat pump and building energy management system.

Two separate interfaces are designed for AC and DC connections, i.e. for PV and grid connection respectively, which are shown in Fig. 5. In order to prevent any negative interaction between two DC sources, the voltage of PV interface is 10 V higher than the DC bus from the grid. In addition, this voltage difference automatically gives the priority to the dominated interface, i.e. PV power, as long as the solar irradiation is enough.

During the periods when there is no cooling demand, i.e. moderate days, or when the tank is fully charged, the surplus energy could be delivered to the building through an inverter. The building inverter is shown in Fig. 1. Grid feed-in was not possible at the demonstration site but domestic electrical consumption of building was far more than the PV power, which guaranteed enough electrical demand.

Table.1.
Technical Data of the Water/Water Heat Pump from Heliotherm

Heating capacity	***15.07 kW***
Cooling capacity*	12.93 kW
Electrical power	2.14 kW
COP	7.06
Compressor Type	Scroll
Compressor Speed	1200-5400 min-1
Refrigerant	R410a

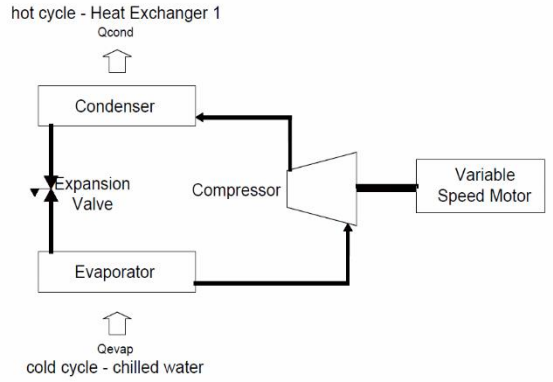

Fig. 4. Schematic diagram of VSHP

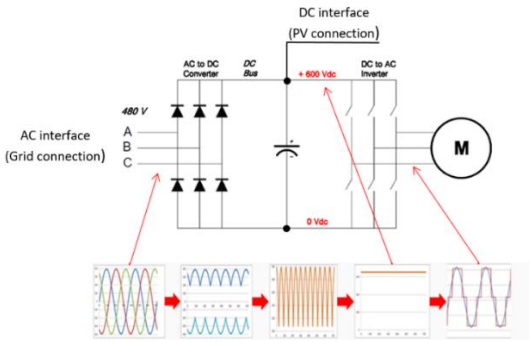

Fig. 5. VFD internal circuit and output of each stage. The final output is a "rectangular" wave form with desired frequency which is compared with a similar sinusoidal wave [25].

4. System performance assessment

Performance assessment includes building cooling demand measurements, available solar energy simulation and measurement and heat pump performance monitoring. A web-based data acquisition system gathers the required information by using more than 40 sensors. A list of the most important sensors is presented in Table 2. Water temperature is measured every 5 minutes by PT1000 sensors with permissible error of ±0.75 °C. Weather data is gathered every 5 seconds through a data logging device. The power is calculated based on the current and voltage measurement with accuracy of 0.9 % and 1 % respectively. Compressor speed is measured by the integrated sensor of the heat pump. Accuracy of this sensor is 1.5 % according to the manufacture data.

Table.2.
List of instrumentation and monitoring sensors

Cooling demand measurement	***Solar energy measurement***
Floor cooling system Water temperature- forward and return flow	Daily horizontal irradiance
ventilation system Water temperature- forward and return flow	DC current of inverter
Floor cooling system water flow	AC current of inverter
ventilation system water flow	DC Voltage of inverter
Labs and offices air temperature	AC Voltage of inverter
Ambient temperature and humidity	UV-Index

A) Building cooling demand

There are three types of cooling loads in the building: a ventilation system which provides conditioned fresh air for laboratories, a floor cooling system for offices and chilled water for lab machines. Details of these loads are depicted in Fig. 6. The machine cooling load is excluded from simulation and measurement because its demand does not follow any predictable patterns and the main goal of the project is to design a cooling system for "usual" buildings. The building cooling demand is monitored since 2019.

B) Available solar energy

Although south-faced is the optimum installation direction for panels, according to the building direction and the space limitation on the roof, either southeast (SE) or southwest (SW) faced could be opted. Consequently, annual solar radiation drops from 3.37 (kWh/m^2/day) to 3.20 and 3.22 (kWh/m^2/day) respectively which is about 5%. Energy reduction for both directions is almost equal but simulation results show that by installing the panels in SW direction, maximum power occurs after midday whereas for SE direction happens before midday. According to the building cooling demand, it would be better to shift the solar power peak to the afternoon. Therefore, SW direction matches better with the project goals. Fig. 7 shows solar energy curves of August 19th for both directions. Energy harvesting is same in both cases, but the power peak is shifted by about two hours.

C) Performance of heat pump

In order to provide preliminary information for control system, the heat pump was operated without application of the PV system. An adjustable DC power supplier was used to provide DC current with different powers to run the heat pump. The data including the rotation speed of the compressor,

temperature difference and flow rate of both heating side (condenser) and cooling side (evaporator) were measured and recorded. From the recorded data, heating and cooling power at different rotation speeds of the compressor were calculated. The data containing the correlation between the rotation speed of compressor (RPMs) and the cooling power, also temperature difference of heating side (condenser) are displayed in Fig. 8. Temperature difference on the heating side (condenser) lies around 2.8 – 6.7K. The reason of such a wide range is the

complex configuration and high temperature inertia on the heating side, i.e. heat should be removed from the heat pump condenser to the hot water cycle. This heat will be transferred to glycol through the heat exchanger 1 (see Fig. 1), then glycol exchanges the heat with ambient air in the air/glycol cooler on the roof. The water pump, glycol pump and the fan of the air/glycol cooler should be adjusted to provide the desired temperature difference ($\Delta T_{desired}$ = 5 K) which is challenging. The range of temperature difference. On the cooling side (evaporator) is quite better due to the simple configuration on this side, it lies around 3.3 – 5.8K. As shown in Fig. 8, cooling power lies in the range from 9.2 to 16.3 kW. As the rotation speed of the compressor increases, the amount of thermal power also increases. Operating data of heat pump are shown in Table 3.

D) Performance test of whole configuration

The components, including PV system, inverter, heat pump and the building piping system, were tested during the summer of 2020 for a period of 14 weeks. The data of the 4th week, between June 19th and June 25th, was used to calculate the system performance. This period is selected because while the average solar irradiance of this week was close to the average of the whole season, the ambient temperature and cooling degree-days (CDD) of the selected week was higher than for the other weeks. Therefore, this week could be referred as the worst-case scenario and the overall performance of the system is better or at least equal to the reference week. The average of daily Global Horizontal Irradiance of the whole period and the reference week are 361 and 382 Wh m^{-2} respectively. Whilst the cooling degree-days of the reference week is 4.03, which is significantly higher than the average value, i.e. 1.71. Fig. 9 shows the temperature and cooling degree-days of different weeks of the cooling season in 2020.

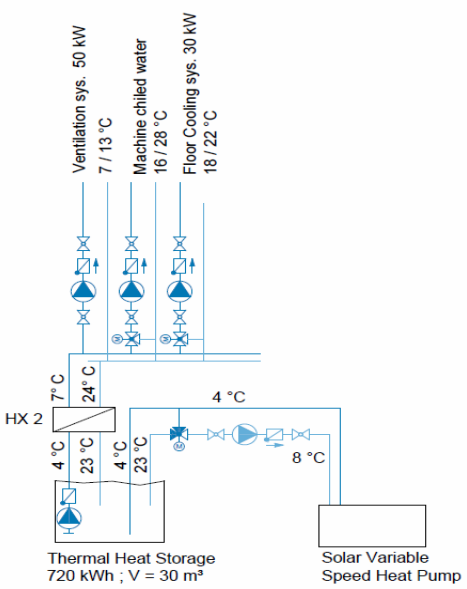

Fig. 6. Details of different cooling loads in the building including ventilation system, floor cooling system and chilled water for processes.

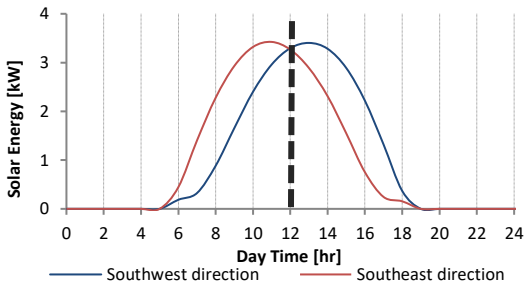

Fig. 7. Solar energy harvesting on 19th of August for SW and SE direction is shown. The peak is shifted from 11:00 to 13:00 by changing the direction to SW, which could match better with cooling demand.

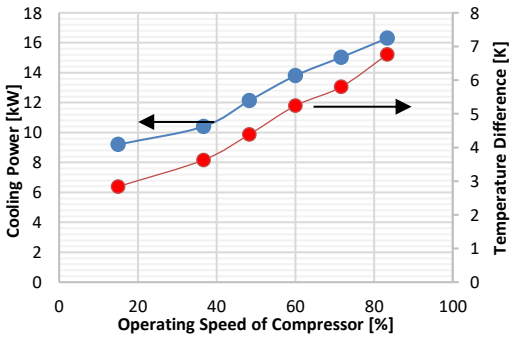

Fig. 8. Cooling power of heat pump (blue curve) and Temperature difference on the heating side, condenser (red curve) in different compressor speed.

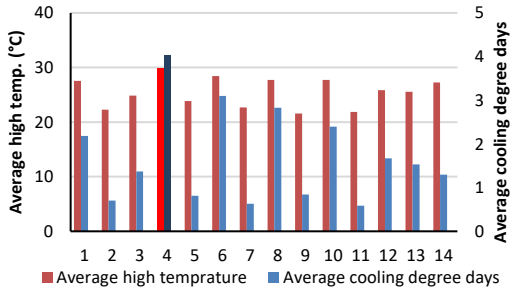

Fig. 9. Weather condition of the demonstration site between 29.05.2020 and 31.08.2020. The reference week, i.e. 4th week, has the highest temperature and cooling degree-days.

Table.3.
Range of operating data of Heat Pump; compressor speed lies between 10 and 83 percent.

Input water Temp.- cooling side (°C)	11.4
Input water Temp.- heating side (°C)	38.4
Cooling power (kW)	9.2 - 16.3
Rejected heat (kW)	7.9 – 18.9
Electric power consumption(kW)	2.7-5.8
temperature diff. of heating side (K)	2.8 – 6.7
temperature diff. of cooling side (K)	3.3 – 5.8
COP	3.4- 2.8

The energy stream of the heat pump is depicted for June 20th in Fig. 10. Most of the day, the heat pump is powered by solar energy and the grid just provides the base energy. In this condition, the heat pump doesn't follow the building cooling demand and it changes according to the available solar energy, extra cooling power will be stored in the tank for the overnight demand or for next day. Between 15:30 and 16:30 there is a reduction in PV power because of clouds shading, which is compensated by grid power immediately. Fig. 11 illustrates the compressor speed for the same day. As mentioned before, intermittency of PV power is transferred to compressor speed. The speed fluctuations are compensated by the storage tank.

Fig. 12 shows the heat pump energy stream for June 22nd, when average cloud coverage was above 50 %. Before noon, PV power is not available. Therefore, the heat pump is fed by the grid and it follows the building cooling load. Cooling demand is low in the morning but it increases with time. After noon, solar energy was available in some periods. Through these durations, inverter gives the priority to the PV power and reduces the grid input. After 2:20pm, the solar irradiation exceeds the building cooling load, but the heat pump follows the available solar energy and continues with the maximum possible speed. The surplus energy will be stored in the tank, which can be used in the afternoon.

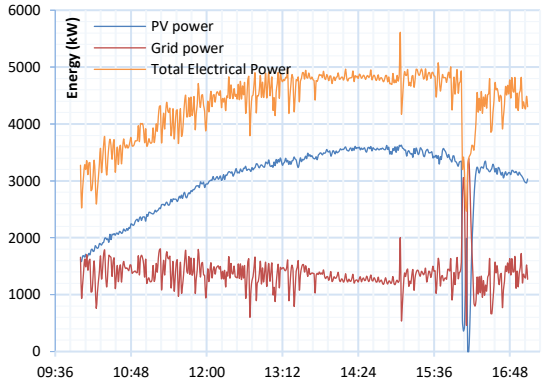

Fig. 10. Energy stream of heat pump for June 20th. Reduction in PV power is compensated by increasing grid power and reducing compressor speed.

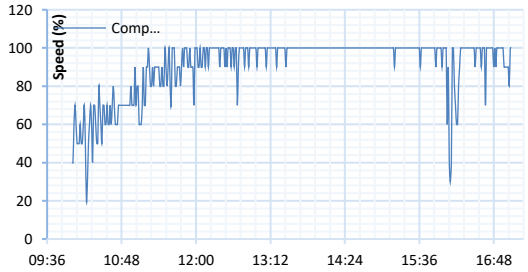

Fig. 11. Compressor speed for June 20th. Heat pump works at full speed regardless of building cooling demand in order to increase the solar fraction of system.

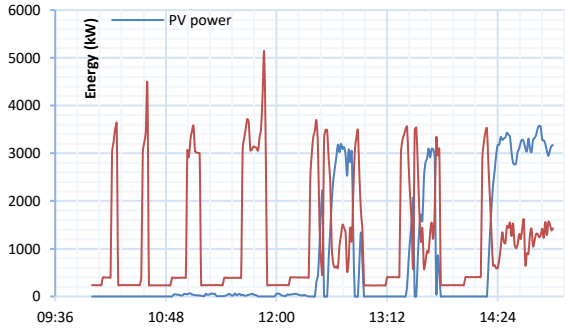

Fig. 12. Energy stream in a cloudy day (June 22nd). When solar energy is deficient, the heat pump will be fed by grid power and follows the building load. When solar energy is available, heat pump will be powered by PV and follows the solar energy curve.

This control strategy increases the solar fraction significantly. Solar fraction is calculated according to the ratio of input PV power to the total input energy including PV and grid.

$$solar\ fraction = \frac{PV\ power}{PV\ power + Grid\ power} \quad (1)$$

Solar fraction for June 20th with average cloud coverage of 24% and for June 22nd with average cloud coverage of 52% is calculated as 68.7% and 20% respectively. The variations of total electrical power and power generated by PV system for June

20th is also presented in Fig. 10. There are two main reasons for such a high SF; (1) the fast contribution between PV and grid power without any auxiliary backup system. (2) The compressor can work at very low speed, almost 10% of its nominal speed, which increases the using of solar energy.

5. Conclusion

One of the main challenges solar air conditioning applications face, is lack of demonstrating systems with high efficiency. In this project, the technical feasibility of utilizing a novel electrically driven solar-assisted cooling system was investigated. The performance of the whole system including the PV system, inverter, heat pump and piping system was studied for the hottest week of the year. The result shows that the proposed cooling system can reduce the electricity consumption around 69% on a sunny day. The variable speed heat pump enables a high system efficiency and is directly powered by DC current. Thus, the energy transformation related energy losses can be substantially decreased. In addition, through a separate AC interface, the system could be fed by grid power when needed without any back up system. This work proved that the proposed concept is technically feasible and has a high energy saving potential. However, more optimizations are possible;

- The base energy is provided by grid, which could be optimized to increase the SF.
- Forecasting software could be used to limit the grid consumption just to the off-peak periods.
- Feed-in strategies could be added to the control system.

References

[1] M. Qu, H. Yin, D.H. Archer, A solar thermal cooling and heating system for a building: Experimental and model based performance analysis and design, Solar Energy, 84 (2) (2010) 166-182.

[2] F.J. Aguilar, P.V. Quiles, S. Aledo, Operation and Energy Efficiency of a Hybrid Air Conditioner Simultaneously Connected to the Grid and to Photovoltaic Panels, Energy Procedia, 48 (2014) 768-777.

[3] P. Bermejo, F.J. Pino, F. Rosa, Solar absorption cooling plant in Seville, Solar Energy, 84 (8) (2010) 1503-1512.

[4] A. Al-Alili, Y. Hwang, R. Radermacher, I. Kubo, Optimization of a solar powered absorption cycle under Abu Dhabi's weather conditions, Solar Energy, 84 (12) (2010) 2034-2040.

[5] F. Cascetta, L. Cirillo, A. Corte, S. Nardini, Comparison between different solar cooling thermally driven system solutions for an office building in Mediterranean Area, 2017.

[6] B.H. Gebreslassie, G. Guillén-Gosálbez, L. Jiménez, D. Boer, A systematic tool for the minimization of the life cycle impact of solar assisted absorption cooling systems, Energy, 35 (9) (2010) 3849-3862.

[7] B.J. Huang, J.H. Wu, R.H. Yen, J.H. Wang, H.Y. Hsu, C.J. Hsia, C.W. Yen, J.M. Chang, System performance and economic analysis of solar-assisted cooling/heating system, Solar Energy, 85 (11) (2011) 2802-2810.

[8] M. Muzaffar, F. Ghaith, Design and simulation of solar powered cooling system in UAE, in: International Conference On Future Trends In Structural, Civil, Environmental and Mechanical Engineering, Thailand, 2013.

[9] M. Pons, G. Anies, F. Boudehenn, P. Bourdoukan, J. Castaing-Lasvignottes, G. Evola, A. Le Denn, N. Le Pierrès, O. Marc, N. Mazet, D. Stitou, F. Lucas, Performance comparison of six solar-powered air-conditioners operated in five places, Energy, 46 (1) (2012) 471-483.

[10] N.U. Rather, R. Rather, S. K Singh, U. Nazir, Performance evaluation and COP calculation of Triple effect vapour Absorption machine working on Solar Thermal energy, 2018.

[11] T. Otanicar, R.A. Taylor, P.E. Phelan, Prospects for solar cooling – An economic and environmental assessment, Solar Energy, 86 (5) (2012) 1287-1299.

[12] N. Hartmann, C. Glueck, F.P. Schmidt, Solar cooling for small office buildings: Comparison of solar thermal and photovoltaic options for two different European climates, Renewable Energy, 36 (5) (2011) 1329-1338.

[13] K.F. Fong, T.T. Chow, C.K. Lee, Z. Lin, L.S. Chan, Comparative study of different solar cooling systems for buildings in subtropical city, Solar Energy, 84 (2) (2010) 227-244.

[14] U. Eicker, D. Pietruschka, A. Schmitt, M. Haag, Comparison of photovoltaic and solar thermal cooling systems for office buildings in different climates, Solar Energy, 118 (2015) 243-255.

[15] J. Sun, H. Yin, F. Wang, Net private benefits of purchasing eco-labeled air conditioners and subsidization policies in China, Energy Policy, 73 (2014) 186-195.

[16] http://www.hvacrbusiness.com/advantages-of-variable-speed-technology.html,

[17] F. Calise, M. Dentice d'Accadia, R.D. Figaj, L. Vanoli, A novel solar-assisted heat pump driven by photovoltaic/thermal collectors: Dynamic simulation and thermoeconomic optimization, Energy, 95 (2016) 346-366.

[18] L. Dai, S. Li, L. DuanMu, X. Li, Y. Shang, M. Dong, Experimental performance analysis of a solar assisted ground source heat pump system under different heating operation modes, Applied Thermal Engineering, 75 (2015) 325-333.

[19] Y. Li, B.Y. Zhao, Z.G. Zhao, R.A. Taylor, R.Z. Wang, Performance study of a grid-connected photovoltaic powered central air conditioner in the South China climate, Renewable Energy, 126 (2018) 1113-1125.

[20] S. Sichilalu, H. Tazvinga, X. Xia, Optimal control of a fuel cell/wind/PV/grid hybrid system with thermal heat pump load, Solar Energy, 135 (2016) 59-69.

[21] C. Tzivanidis, E. Bellos, G. Mitsopoulos, K.A. Antonopoulos, A. Delis, Energetic and financial evaluation of a solar assisted heat pump heating system with other usual heating systems in Athens, Applied Thermal Engineering, 106 (2016) 87-97.

[22] ZHAO, ZHIGANG, Photovoltaic air conditioning system, in: U.S.P.a.T.O. (USPTO) (Ed.), United States, 2016.

[23] S. ZHUO, X. MA, J. YOU, F. LI, J. ZHANG, Photovoltaic Air-conditioning System and Photovoltaic Air Conditioner Having Same in: U.S.P.a.T.O. (USPTO) (Ed.), United States 2017.

[24] R.S. Adhikari, N. Aste, M. Manfren, D. Marini, Energy Savings through Variable Speed Compressor Heat Pump Systems, Energy Procedia, 14 (2012) 1337-1342.

[25] http://www.vfds.com,

[26] Tanveer Ahmad , Dongdong Zhang , A critical review of comparative global historical energy consumption and future demand: The story told so far , ELSEVIER 2020

[27] MokhtarGhodbane,BoussadBoumeddane,KhadijaLahrech, Solar thermal energy to drive ejector HVAC systems: A numerical study under Blida climatic conditions , , ELSEVIER 2021 .

[28] Aiman Albatayneh , Mustafa Jaradat , Murad Al-Omary , Maha Zaquot , , Evaluation of Coupling PV and Air Conditioning vs. Solar Cooling Systems—Case Study from Jordan , , MDPI 2021 .

[29] QudamaAl-Yasiri, MártaSzabó , MüslümArıcı , A review on solar-powered cooling and air-conditioning systems for building applications , ELSEVIER 2022 .